Simulation of quantum dot based single-photon sources using the Schrödinger-Poisson-Drift-Diffusion-Lindblad system

Markus Kantner, Thomas Koprucki, Hans-Jürgen Wünsche and Uwe Bandelow

Weierstrass Institute for Applied Analysis and Stochastics
Mohrenstr. 39, 10117 Berlin, Germany
Email: kantner@wias-berlin.de

***Abstract*—The device-scale simulation of electrically driven quantum light sources based on semiconductor quantum dots requires a combination of the (semi-)classical semiconductor device equations with cavity quantum electrodynamics. We present a comprehensive quantum-classical simulation approach that self-consistently couples the (semi-)classical drift-diffusion system to a Lindblad-type quantum master equation. This allows to describe the spatially resolved carrier transport in complex, multi-dimensional device geometries along with the fully quantum-mechanical light-matter interaction in the quantum dot-cavity system. The latter gives access to important quantum optical figures of merit, in particular the second-order correlation function of the emitted radiation. In order to account for the quantum confined Stark effect in the device's internal electric field, the system is solved along with a Schrödinger–Poisson problem, that describes the envelope wave functions and energy levels of the quantum dot carriers. The approach is demonstrated by numerical simulations of a single-photon emitting diode.**

***Keywords*—Single-photon sources, quantum-confined Stark effect, device simulation, quantum-classical coupling**

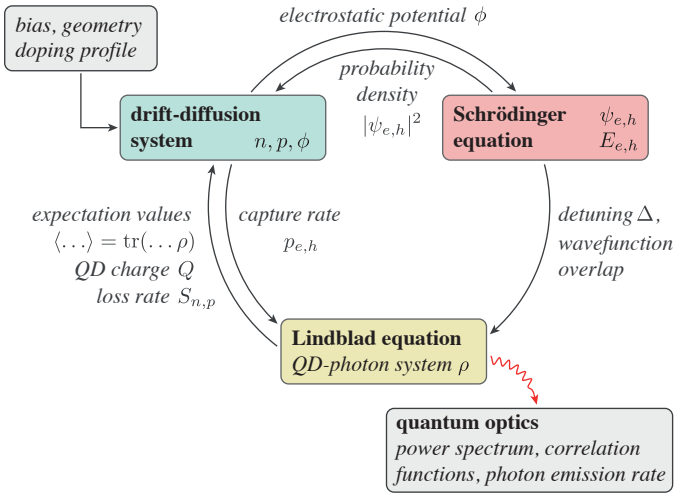

Fig. 1. Schematic illustration of the building blocks and the coupling structure of the Schrödinger–Poisson-Drift-Diffusion-Lindblad system (1)–(5). Adapted, with permission, from Ref. [3]. © SPIE 2019

I. Introduction

The currently unfolding "second quantum revolution" aims at the development of novel quantum technologies that exploit inherent quantum mechanical phenomena for communication and information processing tasks. Many applications, such as eavesdropping-secure encryption methods and optical quantum computers, rely on efficient quantum light sources that emit single photons on demand [1]. Semiconductor quantum dots (QDs) are promising optically active elements for such devices, as they provide an atom-like discrete energy spectrum and can be directly integrated into semiconductor-based photonic resonators by standard growth techniques. In the interest of compactness and scalability, electrical carrier injection is highly desirable to overcome the need for external excitation lasers. The theoretical analysis of the (semi-)classical carrier transport in quantum light emitting diodes can contribute significantly to their optimization, as the numerical simulation facilitates the understanding of counter-intuitive phenomena like rapid spreading of the injection current, which arise under the typically extreme operation conditions (cryogenic temperatures, very low current densities) [2].

On the step from basic research to real world applications, mathematical modeling and numerical simulation can assist the development and optimization of novel device designs. In many well-established simulation tools for optoelectronic devices (e. g., conventional laser diodes, LEDs etc.), the drift-diffusion model is coupled with semi-classical models for the light-matter interaction (e. g., Maxwell–Bloch equations, rate equations) to describe the optically active region. For devices operating in the quantum optical limit, however, fully quantum mechanical models are required to describe the light-matter interaction [4]. To meet this requirement, we have developed a hybrid quantum-classical model system [5], that self-consistently couples the drift-diffusion system to a Lindblad-type quantum master equation [6], which describes the microscopic QD-cavity system in second quantization (dissipative Jaynes–Cummings model). In this paper, we extend our approach by including a self-consistent Schrödinger–Poisson problem, to account for the energy shifts of the bound QD carriers in the device's internal electrostatic field via the quantum confined Stark effect.

978–1–7281–0940–4/19/$31.00 ©2019 IEEE

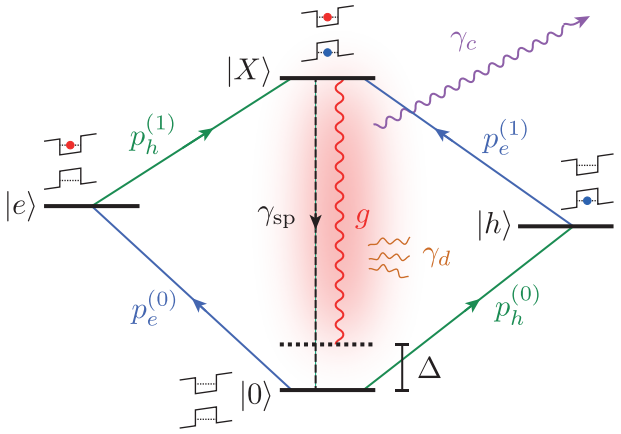

Fig. 2. QD-photon system described by a dissipative Jaynes–Cummings model with 4 electronic states: empty QD $|0\rangle$, single electron $|e\rangle = e^\dagger|0\rangle$, single hole $|h\rangle = h^\dagger|0\rangle$ and bright exciton $|X\rangle = h^\dagger e^\dagger|0\rangle$. The detuning Δ between the exciton energy and the cavity resonance is controlled by the device's internal electrostatic field. Adapted, with permission, from Ref. [3]. © SPIE 2019

II. Hybrid quantum-classical modeling approach

We describe a comprehensive modeling approach for the simulation of quantum light emitting diodes. The approach is based on the hybrid quantum-classical model system proposed in Ref. [5] and is extended by a self-consistent Schrödinger–Poisson problem modeling the envelope wave functions and energy levels of the QD carriers [3]:

$$-\nabla\cdot\varepsilon\nabla\phi = q\,(C+p-n)+Q, \tag{1}$$

$$\partial_t n - \frac{1}{q}\nabla\cdot\mathbf{j}_n = -R - S_n, \tag{2}$$

$$\partial_t p + \frac{1}{q}\nabla\cdot\mathbf{j}_p = -R - S_p, \tag{3}$$

$$H_\alpha^0\psi_\alpha = E_\alpha\psi_\alpha \qquad (\alpha\in\{e,h\}), \tag{4}$$

$$\partial_t\rho = -\frac{i}{\hbar}\,[\mathcal{H},\rho] + \mathcal{D}\rho. \tag{5}$$

The system comprises the semiconductor device equations (1)–(3) for the transport and recombination dynamics of the quasi-free electrons and holes, a stationary one-particle Schrödinger equation (4) for each the QD bound electrons and holes, respectively, and a Lindblad-type quantum master equation (5) for the quantum statistical operator ρ. A schematic illustration of the "Schrödinger-Poisson-Drift-Diffusion-Lindblad system" (1)–(5) and the interconnection of its building blocks is shown in Fig. 1.

A. Semiconductor device equations

The electrostatic interaction between the freely moving and bound carriers of the system is described by Poisson's Eq. (1), where ϕ is the electrostatic potential, n and p are the densities of (continuum) electrons and holes, C is the doping profile, Q is the charge density of the QD carriers, q is the elementary charge and ε is the material's dielectric constant. The carrier densities are related to the electrostatic potential ϕ and the quasi-Fermi energies $\mu_{c/v}$ by the state equations

$$n = N_c F_{1/2}\left(\frac{\mu_c+q\phi-E_c}{k_BT}\right), \quad p = N_v F_{1/2}\left(\frac{E_v-q\phi-\mu_v}{k_BT}\right),$$

where k_B is Boltzmann's constant, T is the absolute temperature, $E_{c/v}$ and $N_{c/v}$ denote the band edge energy and effective density of states of the conduction band/ valence band, respectively, and $F_{1/2}$ is the Fermi–Dirac integral. The current densities $\mathbf{j}_{n/p}$ (3) are driven by the gradients of the quasi-Fermi energies

$$\mathbf{j}_n = M_n n\nabla\mu_c, \qquad \mathbf{j}_p = M_p p\nabla\mu_v,$$

where $M_{n/p}$ denotes the respective mobilities. The (net-)recombination rate R includes spontaneous emission, Shockley–Read–Hall and Auger recombination processes [7].

B. Schrödinger equation and wave function model

The energy levels and (envelope) wave functions of the QD carriers are determined by the stationary Schrödinger equation (4), where the Hamiltonian

$$H_\alpha^0 = -\frac{\hbar^2}{2}\nabla\cdot\frac{1}{m_\alpha^*}\nabla + U_\alpha \pm q\phi, \quad \alpha\in\{e,h\}, \tag{6}$$

involves a position-dependent effective mass m_α^*, the QD confinement potential U_α and the electrostatic potential ϕ given by Eq. (1). The confinement potential combines a finite potential barrier (in growth direction) and a harmonic in-plane confinement as typically assumed for lens-shaped InGaAs-QDs [8]. The Schrödinger Eqs. (4) are solved with outgoing wave conditions on a subset $\Omega_0\subset\Omega$ of the full domain. In general, this is a non-Hermitian eigenvalue problem that yields complex eigenvalues $E_\alpha\in\mathbb{C}$ (quasi-bound states).

C. Lindblad master equation

The many-body Hamiltonian $\mathcal{H}$ in the quantum master Eq. (5) describes the one-particle energy contributions of the QD carriers, the energy of the quantized radiation field, the quantum-mechanical light-matter interaction and the Coulomb interaction between the bound carriers in second quantization:

$$\begin{aligned}\mathcal{H} = {}& \varepsilon_e e^\dagger e + \varepsilon_h h^\dagger h + \hbar\omega_0 a^\dagger a \\ & + \hbar g\left(e^\dagger h^\dagger a + a^\dagger h e\right) - V_{e,h} e^\dagger h^\dagger h e.\end{aligned} \tag{7}$$

Here, a and $a^\dagger$ are the bosonic annihilation and creation operators of the cavity photons and e (h) and $e^\dagger$ ($h^\dagger$) are the respective fermionic operators for the QD-bound electrons (holes). The single-particle energies $\varepsilon_{e/h} = \mathrm{Re}\left(E_{e/h}\right)$ are taken as the real values of the complex eigenvalues determined by Eq. (4). Moreover, $\hbar\omega_0$ is the resonance energy of the cavity and

$$g = d_{c,v}\sqrt{\frac{\omega_0}{\hbar\varepsilon_0 n_r^2 V_0}}\int_{\Omega_0}\mathrm{d}^3r\,\psi_e^*(\mathbf{r})\,\psi_h(\mathbf{r})$$

is the light-matter coupling constant with the interband dipole moment $d_{c,v}$, mode volume V_0 and refractive index n_r. Finally, $V_{e,h}$ is the QD exciton binding energy.

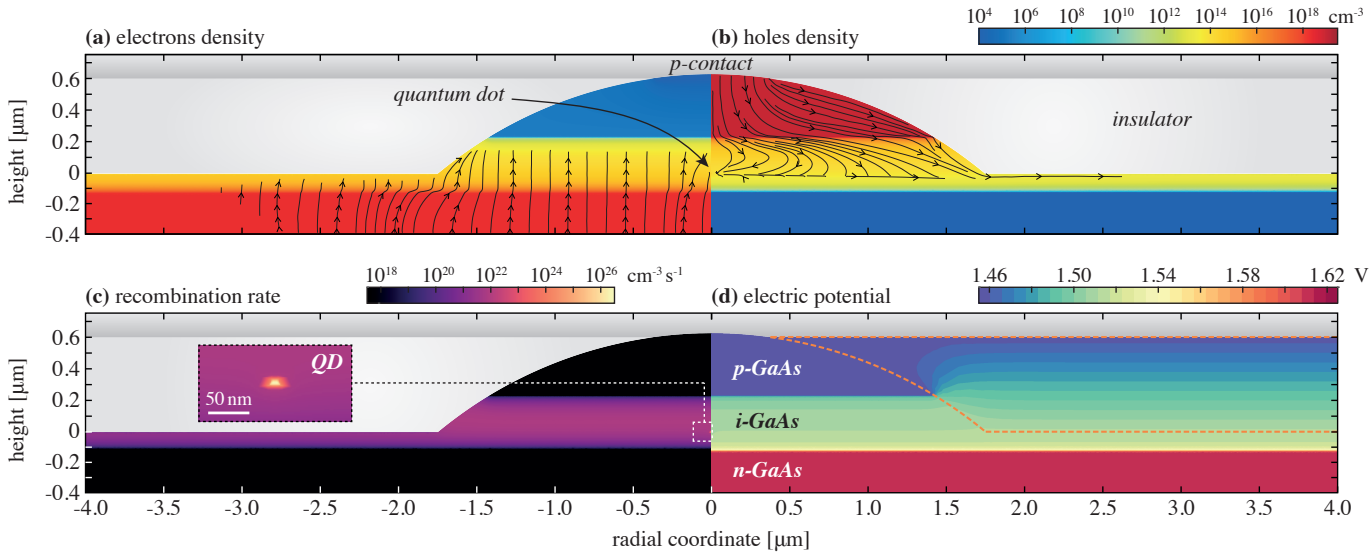

Fig. 3. Stationary injection at $I = 2.75\,\mathrm{nA}$ ($U = 1.49\,\mathrm{V}$) and $T = 30\,\mathrm{K}$. The QD is located on the symmetry axis at $(r, z) = (0, 0)$. (a) Electron density n (color coded) and current density $\mathbf{j}_n$ (arrows indicate the direction of particle flux) and (b) hole density p (color coded) and current density $\mathbf{j}_p$. In the low-injection regime, the scattering of continuum carriers to the QD contributes notably to the current guiding. (c) Recombination rate and scattering losses $R + S_n + S_p$ of continuum carriers. (d) Electrostatic potential ϕ in the diode and the insulator domain. Adapted, with permission, from Ref. [3]. © SPIE 2019

The dissipation superoperator $\mathcal{D}(\rho)$ in Eq. (5) models the irreversible coupling of the quantum system to its macroscopic environment. For the sake of coupling to the semiconductor device equations, we separate the full dissipator

$$\mathcal{D}(\rho) = \mathcal{D}_e(\rho) + \mathcal{D}_h(\rho) + \mathcal{D}_0(\rho) \tag{8}$$

into processes that change the charge of the QD ($\mathcal{D}_{e/h}(\rho)$) or leave it invariant ($\mathcal{D}_0(\rho)$). The individual terms are

$$\mathcal{D}_e(\rho) = p_e^{(0)} L_{e^\dagger(1-n_h)}\rho + p_e^{(1)} L_{e^\dagger n_h}\rho, \tag{9a}$$
$$\mathcal{D}_h(\rho) = p_h^{(0)} L_{h^\dagger(1-n_e)}\rho + p_h^{(1)} L_{h^\dagger n_e}\rho, \tag{9b}$$
$$\mathcal{D}_0(\rho) = \gamma_c L_a\rho + \gamma_{\mathrm{sp}} L_{eh}\rho + \gamma_d L_{n_e n_h}\rho \tag{9c}$$

where $L_A\rho = A\rho A^\dagger + \frac{1}{2}\left(A^\dagger A\rho + \rho A^\dagger A\right)$ is the Lindblad superoperator [6]. The capture of electrons and holes into the QD is described by $\mathcal{D}_e(\rho)$ and $\mathcal{D}_h(\rho)$, where $p_{e/h}^{(0)}$ is the capture rate for scattering into an empty QD. If the QD is already charged by a single carrier, the enhanced capture rate $p_{e/h}^{(1)}$ applies. The capture rates are driven by the continuum carrier densities n, p in the vicinity of the QD

$$p_e^{(i)} = \Gamma_e^{(i)} \int_{\Omega_0} \mathrm{d}^3 r\, |\psi_e|^2 n, \quad p_h^{(i)} = \Gamma_h^{(i)} \int_{\Omega_0} \mathrm{d}^3 r\, |\psi_h|^2 p,$$

$i \in \{0, 1\}$, with capture coefficients $\Gamma_{e/h}^{(i)}$ fitted to microscopic calculations. The charge neutral dissipative processes in $\mathcal{D}_0$ are the emission of cavity photons with loss rate γ_c, the spontaneous emission of the QD exciton to waste modes with decay rate γ_{sp} and phenomenological pure dephasing with γ_d.

D. Coupling terms in macroscopic system

Finally, due to charging of the QD and scattering of continuum carriers to bound states, the quantum system couples back to the semi-classical transport system (1)–(3). The QD charge density Q in Poisson's Eq. (1) is given by the expectation value of the field operator $\Psi(\mathbf{r}) = \psi_e(\mathbf{r})\, e + \psi_h^*(\mathbf{r})\, h^\dagger$

$$Q(\rho) = -q\left\langle \Psi^\dagger \Psi \right\rangle \approx q\,|\psi_h|^2 \left\langle h^\dagger h \right\rangle - q\,|\psi_e|^2 \left\langle e^\dagger e \right\rangle, \tag{10}$$

where $\langle \ldots \rangle = \mathrm{tr}(\rho \ldots)$, i.e., the QD carrier's spatial probability distributions (from Eq. (4)) multiplied by the occupation probability obtained from the quantum master equation (5). Following Ref. [5], the loss terms (due to capture of continuum carriers to the QD) on the right hand side of the continuity equations (2)–(3) are modeled using the charge number operator $N = e^\dagger e - h^\dagger h$ and the dissipators (9a)–(9b) as

$$S_n = +|\psi_e(\mathbf{r})|^2\, \mathrm{tr}\left(N\mathcal{D}_e(\rho)\right), \tag{11a}$$
$$S_p = -|\psi_h(\mathbf{r})|^2\, \mathrm{tr}\left(N\mathcal{D}_h(\rho)\right). \tag{11b}$$

The definitions (10)–(11) guarantee charge conservation [3, 5].

III. Numerical Method and Simulation Results

The hybrid quantum-classical model system (1)–(5) is applied to simulate the stationary operation characteristics of the single-photon emitting diode shown in Fig. 3. The diode features a monolithically fabricated microlens structure on top, which is optimized for a high coupling efficiency to an external optical fiber [9]. The top-contact is assumed to consist of an optically transparent material (e. g., ITO), placed on an thick insulator layer with relative permittivity $\varepsilon_s = 3.0$. There is only a small semiconductor-contact interface, see Fig. 3. On the insulator domain, only Poisson's Eq. (1) is solved. The GaAs material parameters for the drift-diffusion system are taken from Ref. [10], the doping densities are assumed as $N_D^+ = 2 \times 10^{18}\,\mathrm{cm}^{-3}$ and $N_A^- = 1 \times 10^{19}\,\mathrm{cm}^{-3}$. Despite the low temperature $T = 30\,\mathrm{K}$, full ionization of the dopants is assumed due to the metal-insulator transition. For the carrier mobilities $M_{n,p}$ a temperature and doping dependent low field

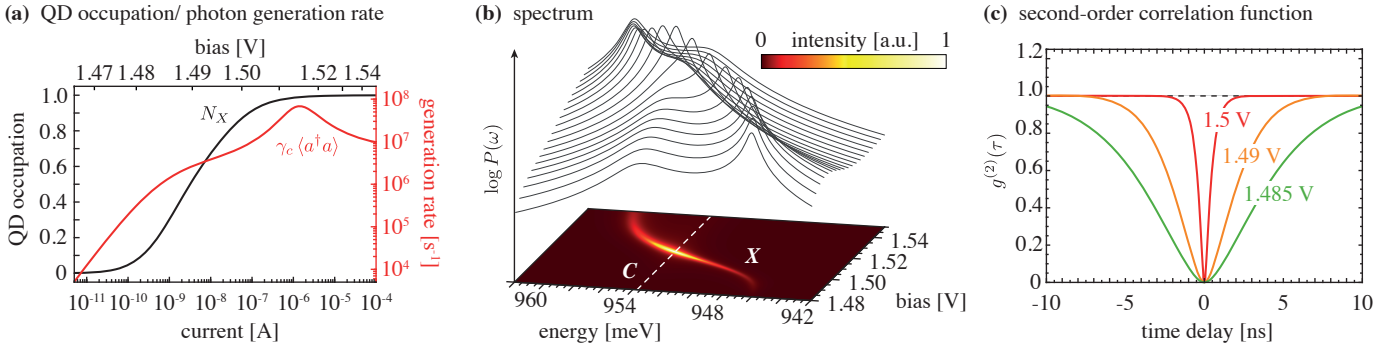

Fig. 4. (a) Exciton occupation probability N_X and photon emission rate $\gamma_c\langle a^\dagger a\rangle$ as a function of the injection current (or applied bias). (b) Power spectrum $P(\omega)$ calculated from Eq. (12) vs. applied bias. The exciton energy (X) is blue-shifted with the increasing bias due to the quantum confined Stark effect. The resonance with the optical cavity mode (C) appears at $U \approx 1.516\,\mathrm{V}$ and yields a maximum photon emission rate of about 70 MHz. (c) Time-resolved second-order correlation function $g^{(2)}(\tau)$ at different applied voltages. Adapted, with permission, from Ref. [3]. © SPIE 2019

model is used [11]. The full system (1)–(5) is solved by iterating (1)–(3)→(4)→(5)→(1)–(3)→ ... until convergence is reached (cf. Fig. 1 (a)). The drift-diffusion system (1)–(3) is discretized using a finite volume Scharfetter–Gummel method for Fermi–Dirac statistics [12, 13]. We use the temperature embedding method described in Ref. [14] to cope with the ill-conditioned discrete system at cryogenic operation temperature and low bias. Schrödinger's Eq. (4) is discretized using a second order finite difference scheme.

Figure 1 (a) shows the QD occupation and photon generation rate as a function of the applied bias. The power spectrum

$$P(\omega) = \frac{1}{2\pi}\int_{-\infty}^{\infty} \mathrm{d}\tau\, e^{-i\omega\tau}\langle a^\dagger(\tau)\, a(0)\rangle \qquad (12)$$

is shown in Fig. 1 (b). At $U \approx 1.516\,\mathrm{V}$ the QD exciton is tuned into resonance with the cavity mode (via the quantum confined Stark effect), which yields a maximum single-photon generation rate of about 70 MHz, see Fig. 1 (a). At high injection currents, excitation-induced dephasing leads to a notable broadening of the emission line. Slightly below the diode's threshold voltage, the loss terms $S_{n/p}$ are the dominant terms on the right hand side of the continuity Eqs. (2)–(3), see Fig. 3 (c), such that the QD appreciably contributes to current guiding, see Fig. 3 (a, b). The second-order correlation function

$$g^{(2)}(\tau) = \frac{\langle a^\dagger(0)\, a^\dagger(\tau)\, a(\tau)\, a(0)\rangle}{\langle a^\dagger(0)\, a(0)\rangle^2} \qquad (13)$$

describes the single-photon purity of the device and is plotted in Fig. 1 (c) for different voltages. The characteristic dip at $g^{(2)}(0) \approx 0$ indicates *anti-bunching* of the emitted photons, which is a truly non-classical feature of the optical field.

IV. Outlook and Conclusions

The hybrid quantum-classical model system for the simulation of electrically driven quantum light sources introduced in Ref. [5] has been extended by a self-consistent Schrödinger–Poisson system. The extended model allows to describe important phenomena such as the quantum confined Stark effect and resonances with the cavity mode. It might be used to investigate spectral diffusion of the emission energy due to stochastic fluctuations in future works.

Acknowledgment

This work was funded by the German Research Foundation (DFG) under Germany's Excellence Strategy – EXC2046: Berlin Mathematics Research Center MATH+ (grant AA2-3).

References

[1] P. Michler, ed., *Quantum Dots for Quantum Information Technologies*. Series in Nano-Optics and Nanophotonics, Cham: Springer, 2017.

[2] M. Kantner, U. Bandelow, T. Koprucki, J.-H. Schulze, A. Strittmatter, and H.-J. Wünsche, "Efficient current injection into single quantum dots through oxide-confined p-n-diodes," *IEEE Trans. Electron Devices*, vol. 63, no. 5, pp. 2036–2042, 2016.

[3] M. Kantner, "Hybrid modeling of quantum light emitting diodes: Self-consistent coupling of drift-diffusion, Schrödinger–Poisson and quantum master equations," *Proc. SPIE*, vol. 10912, p. 109120U, 2019.

[4] W. W. Chow and F. Jahnke, "On the physics of semiconductor quantum dots for applications in lasers and quantum optics," *Prog. Quantum Electron.*, vol. 37, no. 3, pp. 109–184, 2013.

[5] M. Kantner, M. Mittnenzweig, and T. Koprucki, "Hybrid quantum-classical modeling of quantum dot devices," *Phys. Rev. B*, vol. 96, no. 20, p. 205301, 2017.

[6] H.-P. Breuer and F. Petruccione, *The Theory of Open Quantum Systems*. Oxford: Oxford University Press, 2002.

[7] S. Selberherr, *Analysis and Simulation of Semiconductor Devices*. Vienna: Springer, 1984.

[8] T. R. Nielsen, P. Gartner, and F. Jahnke, "Many-body theory of carrier capture and relaxation in semiconductor quantum-dot lasers," *Phys. Rev. B*, vol. 69, p. 235314, Jun 2004.

[9] P.-I. Schneider, N. Srocka, S. Rodt, L. Zschiedrich, S. Reitzenstein, and S. Burger, "Numerical optimization of the extraction efficiency of a quantum-dot based single-photon emitter into a single-mode fiber," *Opt. Express*, vol. 26, no. 7, pp. 8479–8492, 2018.

[10] V. Palankovski and R. Quay, *Analysis and Simulation of Heterostructure Devices*. Series in Computational Microelectronics, Vienna: Springer, 2004.

[11] M. Sotoodeh, A. H. Khalid, and A. A. Rezazadeh, "Empirical low-field mobility model for III-V compounds applicable in device simulation codes," *J. Appl. Phys.*, vol. 87, no. 6, pp. 2890–2900, 2000.

[12] T. Koprucki, N. Rotundo, P. Farrell, D. H. Doan, and J. Fuhrmann, "On thermodynamic consistency of a Scharfetter–Gummel scheme based on a modified thermal voltage for drift-diffusion equations with diffusion enhancement," *Opt. Quantum. Electron.*, vol. 47, pp. 1327–1332, 2015.

[13] P. Farrell, N. Rotundo, D. H. Doan, M. Kantner, J. Fuhrmann, and T. Koprucki, "Drift-diffusion models," in *Handbook of Optoelectronic Device Modeling and Simulation: Lasers, Modulators, Photodetectors, Solar Cells, and Numerical Methods* (J. Piprek, ed.), vol. 2, ch. 50, pp. 733–771, Boca Raton: CRC Press, Taylor & Francis Group, 2017.

[14] M. Kantner and T. Koprucki, "Numerical simulation of carrier transport in semiconductor devices at cryogenic temperatures," *Opt. Quantum. Electron.*, vol. 48, no. 12, p. 543, 2016.